Correlation between Charge Movement and Ionic Current during Slow Inactivation in *Shaker* K$^+$ Channels

Riccardo Olcese,* Ramón Latorre,*¶ Ligia Toro,*§∥ Francisco Bezanilla,‡∥¶ and Enrico Stefani*‡∥¶**

From the *Department of Anesthesiology, ‡Department of Physiology, §Department of Molecular and Medical Pharmacology, and ∥Brain Research Institute, University of California, Los Angeles, CA 90095-1778; ¶Centro de Estudios Cientificos de Santiago, and Department of Biology, Faculty of Science, University of Chile, Santiago, 9 Chile; and **Conicet, Buenos Aires, 1033 Argentina

ABSTRACT   Prolonged depolarization induces a slow inactivation process in some K$^+$ channels. We have studied ionic and gating currents during long depolarizations in the mutant *Shaker* H4-Δ(6–46) K$^+$ channel and in the nonconducting mutant (*Shaker* H4-Δ(6–46)-W434F). These channels lack the amino terminus that confers the fast (N-type) inactivation (Hoshi, T., W.N. Zagotta, and R.W. Aldrich. 1991. *Neuron.* 7:547–556). Channels were expressed in oocytes and currents were measured with the cut-open-oocyte and patch-clamp techniques. In both clones, the curves describing the voltage dependence of the charge movement were shifted toward more negative potentials when the holding potential was maintained at depolarized potentials. The evidences that this new voltage dependence of the charge movement in the depolarized condition is associated with the process of slow inactivation are the following: (*a*) the installation of both the slow inactivation of the ionic current and the inactivation of the charge in response to a sustained 1-min depolarization to 0 mV followed the same time course; and (*b*) the recovery from inactivation of both ionic and gating currents (induced by repolarizations to −90 mV after a 1-min inactivating pulse at 0 mV) also followed a similar time course. Although prolonged depolarizations induce inactivation of the majority of the channels, a small fraction remains non–slow inactivated. The voltage dependence of this fraction of channels remained unaltered, suggesting that their activation pathway was unmodified by prolonged depolarization. The data could be fitted to a sequential model for *Shaker* K$^+$ channels (Bezanilla, F., E. Perozo, and E. Stefani. 1994. *Biophys. J.* 66:1011–1021), with the addition of a series of parallel nonconducting (inactivated) states that become populated during prolonged depolarization. The data suggest that prolonged depolarization modifies the conformation of the voltage sensor and that this change can be associated with the process of slow inactivation.

KEY WORDS: gating current • potassium current • charge movement

INTRODUCTION

Upon depolarization, the macroscopic conductance increases and then shows a progressive decay. The reduction in conductance with time was referred to as inactivation by Hodgkin and Huxley (1952). Depending on the nature of the mechanism involved, the time course of the inactivation process ranges from a few milliseconds (fast inactivation) to several seconds (slow inactivation). To explain the fast inactivation process in Na$^+$ channels from squid giant axon, Armstrong and Bezanilla (1977) proposed the "ball-and-chain" model. In this model, a tethered inactivating particle, the ball, is able to block the ion passage only after channel opening. In *Shaker* K$^+$ channels, fast inactivation is mediated by the first 20 amino acid residues (the ball) that are tethered

in the 60 amino acid residues that lie between the ball and the first transmembrane domain (Zagotta et al., 1989, 1990; Hoshi et al., 1990). Fast inactivation is induced by the binding of the amino terminus of the channel protein to the internal mouth of the pore. Because of the involvement of the amino terminus in this process, fast inactivation is also known as N-type inactivation. During N-type inactivation, the NH$_2$ terminus interacts with the voltage sensor and slows down the return of the gating charge to its resting position upon repolarization (Bezanilla et al., 1991). This slowdown of the charge return prompted by the inactivation process was first observed in Na$^+$ channels and christened "charge immobilization" (Armstrong and Bezanilla, 1977). *Shaker* K$^+$ channels with amino acid residues 6–46 deleted (*Shaker* H4-Δ), lacks fast inactivation (Hoshi et al., 1990) and charge immobilization (Bezanilla et al., 1991).

Slow inactivation, on the other hand, is less understood. Ehrenstein and Gilbert (1966) showed that prolonged depolarizations resulted in a slow reduction of the K$^+$ conductance in squid giant axon. The mo-

lecular mechanism of this process can be studied in *Shaker* K$^+$ channels lacking fast inactivation (*Shaker* H4-Δ) since they show a relatively voltage insensitive slow decrease in channel open probability as a result of prolonged depolarizations (Hoshi et al., 1991; Choi et al., 1991; Yellen et al., 1994; Liu et al., 1996). Since point mutations in the carboxyl terminus of the channel (S6 transmembrane segment) affect slow inactivation, this process is commonly denominated C-type inactivation (Hoshi et al., 1991; López-Barneo et al., 1993) and is produced by a cooperative mechanism (Panyi et al., 1993; Ogielska et al., 1995). However, mutations in regions other than the S6 segment (for example, in the pore region) can also dramatically alter the inactivation time course (López-Barneo et al., 1993; De Biasi et al., 1993). These results strongly suggest the presence of more than one molecular mechanism in determining the rate of channel inactivation. In those cases in which pore (P) residues in K$^+$ channels are involved in determining the inactivation kinetics, the process has been referred to as P-type inactivation (De Biasi et al., 1993).

The present study, previously presented in abstract form (Olcese et al., 1994, 1995), further investigated the nature of the effect of prolonged depolarization on the ionic conductance and correlates these effects on ionic current with effects on gating current in the *Shaker* H4-Δ K$^+$ channel. Prolonged depolarization produced changes in the voltage dependence of the charge movement similar to the ones described by Bezanilla et al. (1982) for the Na$^+$ channel in squid giant axon. Charge immobilization, as a consequence of long depolarization, has also been reported for the human K$^+$ channel Kv1.5 (Fedida et al., 1996).

MATERIALS AND METHODS

Molecular Biology and Oocyte Injection

cDNA encoding for *Shaker* H4 K$^+$ channel (Kamb et al., 1987) lacking the amino acids 6–46 to remove the fast inactivation (*Shaker* H4-Δ) was used for measurements of ionic and gating currents (Hoshi et al., 1990). For gating current measurements in the corresponding nonconducting mutant, the mutant *Shaker* H4-Δ W434F (Perozo et al., 1993) was used.

24 h before cRNA injection, *Xenopus laevis* oocytes (stage V–VI) were treated with collagenase (200 U/ml; GIBCO BRL, Gaithersburg, MD) in a Ca^{2+}-free solution to remove the follicular layer. Oocytes were injected with 50 nl cRNA 1 μg/μl suspended in water using a "nano-injector" (Drummond Scientific Co., Broomall, PA) and maintained at 18°C in modified Barth's solution containing (mM): 100 NaCl, 2 KCl, 1.8 CaCl$_2$, 1 MgCl$_2$, 5 Na-HEPES (pH 7.6), and 50 mg/ml gentamicin.

Gating and Ionic Current Recording

Gating and ionic currents were recorded 1–7 d after injection using the cut-open oocyte Vaseline gap voltage clamp (COVG) (Stefani et al., 1994) and conventional cell-attached patch clamp tech-

niques. Methanesulphonic acid (MES)[1] was the main anion in the recording external solutions. In the cut-open oocyte technique, the external solutions were (mM): 107 Na-MES, 2 Ca-(MES)$_2$, 10 Na-HEPES (isotonic Na-MES), 107 K-MES, 2 Ca-(MES)$_2$, 10 Na-HEPES (isotonic K-MES) or 110 *N*-methylglucamine-methanesulphonate (NMG-MES), 2 Ca-(MES)$_2$, 10 NMG-HEPES (isotonic NMG-MES Ca-MES 2). The internal solution contained (mM): 110 K-glutamate, 10 K-HEPES. The oocytes were K$^+$ depleted by internal perfusion of the oocyte with a solution containing (mM): 110 NMG-MES, 10 NMG-HEPES, 10 (NMG)$_2$-EGTA (isotonic NMG-MES). The perfusion (1 ml/h) was attained introducing a 20–50 μm glass pipette connected to a syringe pump in the lower part of the oocyte. Standard solution for the intracellular recording micropipette was (mM): 2,700 Na-MES, 10 NaCl. Low access resistance to the oocyte interior was obtained by permeabilizing the oocyte with 0.1% saponin. For the experiments in cell-attached configuration, after the removal of the vitelline membrane, the oocytes were K$^+$ depleted in a solution containing (mM): 110 CsMES, 2 MgCl$_2$, 10 Cs-HEPES (isotonic Cs-MES). To speed up the intracellular K$^+$ replacement by Cs$^+$, the oocyte membrane was damaged at various places with a thin needle. Patch pipettes were filled with (mM): 110 Cs-MES, 2 CaCl$_2$, 10 Cs-HEPES (isotonic Cs-MES CaCl$_2$ 2). All recording and perfusion solutions were buffered at pH 7.0 with 10 mM HEPES. All experiments were performed at room temperature of 22–24°C.

In most cases, gating currents were recorded unsubtracted. Linear components were analogically compensated at positive potentials (20–40 mV) where the membrane capacity becomes voltage independent. This is also the case in slow-inactivated channels in which the charge–voltage curve was shifted to more negative potentials. P/−4 subtracting protocol (Bezanilla and Armstrong, 1977) from a positive holding potential (20 mV) was used for some of the experiments describing the time course of charge inactivation. The filter frequency was 1/5 the sampling frequency.

Modeling

The model-fitting procedure was implemented using the parameter optimization program SCoP (Simulation Resource, Inc., Barren Springs, MI). We used a state kinetic model, expressed as a system of differential equations, with discrete transitions occurring between states. The transition rates between the horizontal lines of states (see Fig. 10 *A*) were exponential functions of the potential as predicted by the Eyring theory. The vertical transitions are assumed to be voltage independent.

RESULTS

Ionic Current Inactivation

Fig. 1, *A* and *B* shows the time course of the current for *Shaker* H4 and *Shaker* H4-Δ for a series of depolarizing pulses of 50-ms duration. *Shaker* H4 displays a fast decay of the ionic current with a time constant of a few milliseconds (Fig. 1 *A*). In the mutant *Shaker* H4-Δ, under the same experimental conditions and time scale, the ionic current is maintained during the pulse (Fig. 1 *B*). However, in the same deletion-mutant *Shaker* H4-Δ,

---

Shaker H4

A

B   **Shaker H4 -Δ**

3 µA
10 ms

6 µA
10 ms
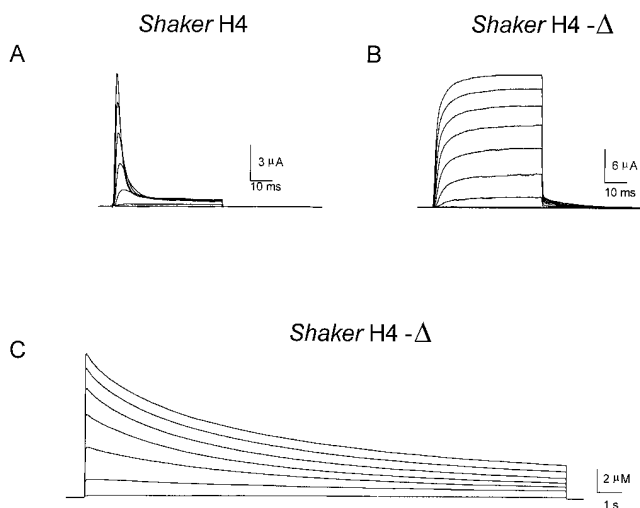
C   **Shaker H4 -Δ**

2 µM
1 s

FIGURE 1. N- and C-type inactivation in *Shaker* channels. (*A*) *Shaker H4*: pulses from −60 to 10 mV in 10-mV steps. Note the fast decay of the K⁺ current due to the N-type inactivation. (*B*) *Shaker* H4-Δ: pulses from −80 to 30 mV in 10-mV steps. The deletion of the amino acids 6–46 (*Shaker H4-Δ*) completely removes the fast inactivating properties of the channel. (*C*) *Shaker* H4-Δ: long pulses (18 s) from −40 to 20 mV in 10-mV steps. Long depolarizing pulses make evident the presence of a slow inactivation process. COVG technique, external isotonic Na-MES.

longer depolarizations make evident a slow inactivation process with a time constant of several seconds (Fig. 1 *C*).

Fig. 2 shows a typical experiment to measure the steady state voltage dependence of the slow inactivation pro-

cess. The experiments were done in isotonic K-MES. To reach the steady state for the slow inactivation process, oocytes were maintained for 1 min at the given holding potential (HP) before the pulse protocol. Fig. 2 *A* shows that the current measured from an HP of −70 mV are larger than those measured at an HP of −30 mV, indicating that the fraction of inactivated channels increases as the holding potential becomes more positive. Fig. 2 *B* illustrates conductance–voltage (G-V) curves obtained from the amplitude of the tail currents at a constant return potential (−50 mV). Membrane conductance (G) was calculated from G = I$_{(-50 mV)}$/(E − E$_K$), where I$_{(-50 mV)}$ is the peak tail current at −50 mV, E$_{(-50mV)}$ is the return potential (−50 mV), and E$_K$ is the K⁺ reversal potential (0 mV in isotonic K-MES). At −50 mV return potential, the slow time course of the tail currents facilitated the peak current determination. Long membrane depolarizations strongly reduce the membrane conductance without significantly changing the voltage dependence of channel opening (Fig. 2, *B* and *C*). Fig. 2 *D* shows the steady state slow inactivation curve. The relative conductance measured as peak tail current at −50 mV for a pulse to −1 mV was plotted as a function of the holding potential, and the data were fitted to a Boltzmann equation that gave a half inactivation voltage of −38.5 mV and an effective valence of 7.2. The holding potential was maintained for 1 min before the test pulse was applied. The curve represents the reduction in availability of K⁺ channels to open as a function
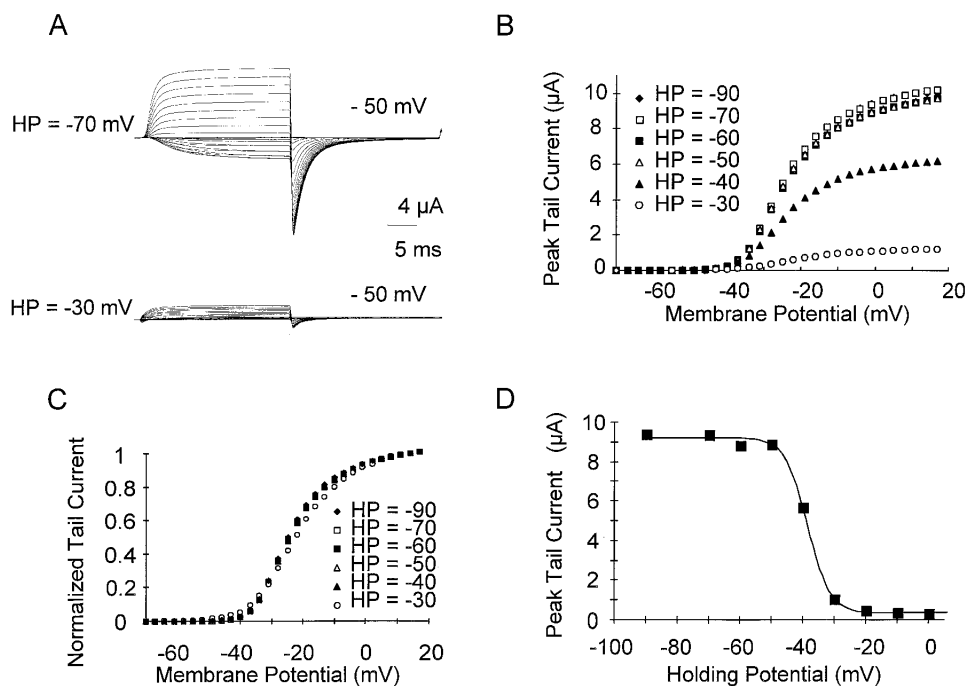
A

HP = -70 mV   − 50 mV

4 µA
5 ms

HP = -30 mV   − 50 mV

B

Peak Tail Current (µA)

◆ HP = -90
□ HP = -70
■ HP = -60
△ HP = -50
▲ HP = -40
○ HP = -30

Membrane Potential (mV)

C

Normalized Tail Current

◆ HP = -90
□ HP = -70
■ HP = -60
△ HP = -50
▲ HP = -40
○ HP = -30

Membrane Potential (mV)

D

Peak Tail Current (µA)

Holding Potential (mV)

FIGURE 2. Steady state inactivation properties of *Shaker* H4-Δ. (*A*) Effect of the HP (−70 and −30 mV) on K⁺ currents recorded with the COVG technique in isotonic K-MES. Pulses between −70 and 17 mV in 3-mV steps from the tested HP were applied. Tail currents were measured at the end of these pulses at a repolarization potential to −50 mV. The oocyte was maintained at each holding potential for 1 min before running the stimulating protocol with low frequency stimulating pulses to prevent their effect on the inactivation (e.g., a pulse every 1 s at −70 mV and every 5 s at 0 mV HPs). Linear components were subtracted after the stimulating run with P/1 from a subtracting holding potential 70 mV more negative than the tested HP and were between −140 and −53 mV with 3-mV increments. (*B*) G-V curves with the protocol shown in *A* from the same oocyte at different HPs: ◆, −90; □, −70; ■, −60; △, −50; ▲, −40; ○, −30 mV. (*C*) Normalized G-V curves. (D) Steady state inactivation curve obtained from tail current amplitude at −50 mV after a depolarizing pulse to −1 mV. Experimental points were fitted to G$_m$ = G$_{min}$ + G$_{max}$/{1 + exp[−z(V$_{1/2}$ − V$_m$)F/RT]}. The fitted values were: G$_{max}$ = 0.17 mS, G$_{min}$ = 0.007 mS, V$_{1/2}$ = −38.5 mV and z = 7.2.

of the membrane depolarization and shows that the steady state inactivation curve is strongly dependent on the holding potential.

Charge Movement from "Slow Inactivated" Channels

Measurements of charge movement make it possible to explore the voltage-dependent characteristics of the different protein conformations that give origin to the closed states that lead to channel opening. We used gating current measurements as a tool to investigate how the activation pathway of the slow inactivated *Shaker* H4-Δ K channels was altered. Using the cut-open oocyte voltage clamp and giant macropatch techniques in K⁺-depleted oocytes, we measured gating current uncontaminated by ionic currents. Oocytes expressing *Shaker* H4-Δ were K⁺ depleted by internal perfusion with NMG-MES (see MATERIALS AND METHODS). Fig. 3, *A* and *B* show selected gating current traces evoked by the indicated pulse potentials, from different holding potentials (−90 mV, Fig. 3 *A* and 0 mV, Fig. 3 *B*). The charge moved during the voltage steps, calculated by integrating the ON gating current, is plotted as a function of the pulse potential (Q-V) in Fig. 3, *C* and *D*. Q-V curves for different holding potentials were constructed from the charge measured immediately after the voltage steps (ON gating current). These measurements should minimize some charge recovery that may occur during repolarizing pulses from depolarized holding

potentials. To obtain a more direct comparison of the Q-V curves obtained with the different holding potentials, in Fig. 3 *D* we have plotted the absolute values of the charge. The total amount of charge that moves in control conditions (−90 mV HP) and after slow inactivation (0 mV HP) is the same. However, the Q-V curve generated by the channels in the inactivated state (0 mV HP) was shifted by ∼50 mV to the left along the voltage axis when compared with the Q-V curve obtained from the noninactivated channels (−90 mV HP). The shift in the Q-V curve indicates that, when the charge returns from the inactivated state after prolonged depolarization, it sees a different energy landscape than the charge moving in normally polarized channels from closed states to the open state. In kinetic terms, this means that the charge movement from the inactivated state does not follow the same kinetic pathway as when the charge moves from the closed to the open state.

Charge Movement after Prolonged Depolarization in the Nonconducting Shaker H4-Δ-W434F

The shift toward more negative potentials of the Q-V curve, induced by long depolarizations, is also present in the nonconducting clone *Shaker* H4-Δ-W434F. For comparison with the conducting clone *Shaker* H4-Δ in the same ionic conditions, oocytes expressing the mutant channel were also K⁺ depleted, and the internal medium replaced with 120 mM NMG-MES. Fig. 4, *A*
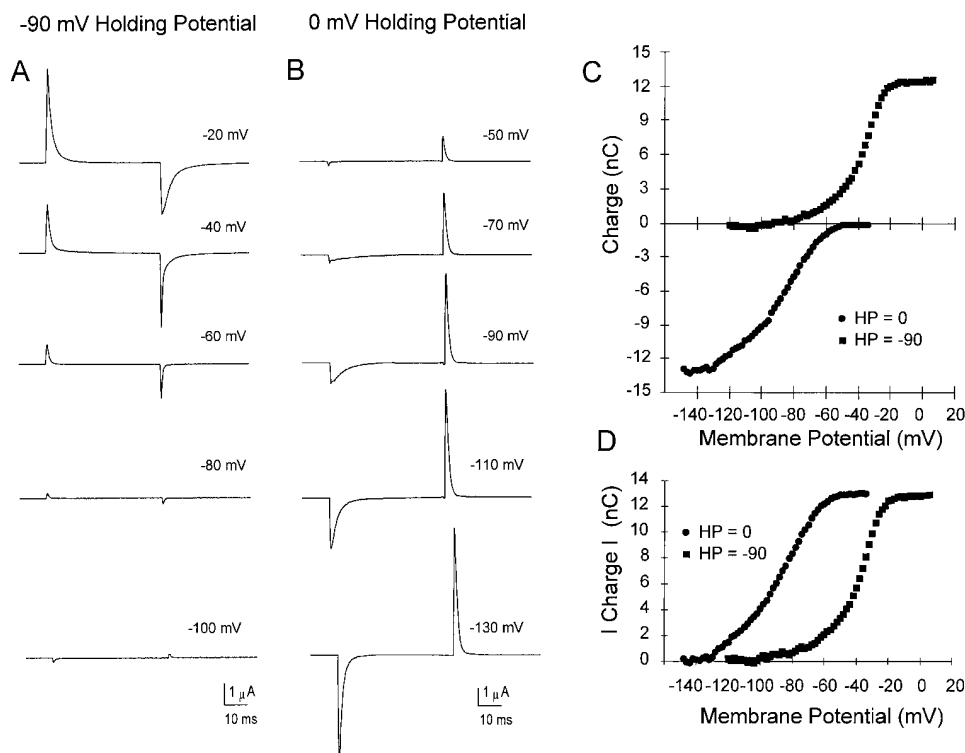

FIGURE 3. Gating currents from −90 and 0 mV HPs in the conducting *Shaker* Δ. The oocyte interior was perfused with isotonic NMG-MES up to the complete elimination of K⁺ currents. The external solution was isotonic NMG-MES Ca-(MES)₂. Unsubtracted gating currents; linear components were analogically compensated with the amplifier transient cancellation at 20 mV HP. (*A* and *B*) Current traces from −90 and 0 mV HP, respectively. The cell was maintained at 0 mV HP for 1 min; pulse stimulation was every 1 s at 0 mV and every 0.5 s at −90 mV HP. (*C*) Q-V curves obtained by integrating the ON gating currents to different test potentials from −90 (■) and 0 (●) mV HP. (D) Q-V curves from *C* replotted defining Q = 0 at the extreme negative potential for both HPs. The total charge moved is the same at both HPs, but holding the membrane potential at 0 mV induces an ∼50-mV shift to more negative potentials of the Q-V curve.

Slow Inactivation in Shaker K⁺ Channels

and *B* show representative gating current traces for the *Shaker* H4-Δ-W434F channel. The traces were recorded during voltage steps to the indicated potentials from −90 (Fig. 4 *A*) and 0 (Fig. 4 *B*) mV holding potential. The Q-V curve of the slow inactivated channels (0 mV HP) is clearly shifted toward more negative potentials compared with that obtained from −90 mV HP (Fig. 4 *C*). The midpoints of the two Q-V curves are ∼25 mV apart. Interestingly, in both the conducting and the nonconducting clones, the voltage dependence of their charge movements when at hyperpolarized potentials was very similar (Bezanilla et al., 1991; compare Figs. 3 *D* and 4 *C*) and both have a left-shifted Q-V curve after a long depolarization. In *Shaker* H4-Δ, the left shift of the Q-V obtained from a holding potential of 0 mV is ∼20 mV more negative than in *Shaker* H4-Δ-W434F.

-90 mV Holding Potential   0 mV Holding Potential

A   **B**

-20 mV   -10 mV

-40 mV   -50 mV

-60 mV   -70 mV

-80 mV   -90 mV

-100 mV   -110 mV

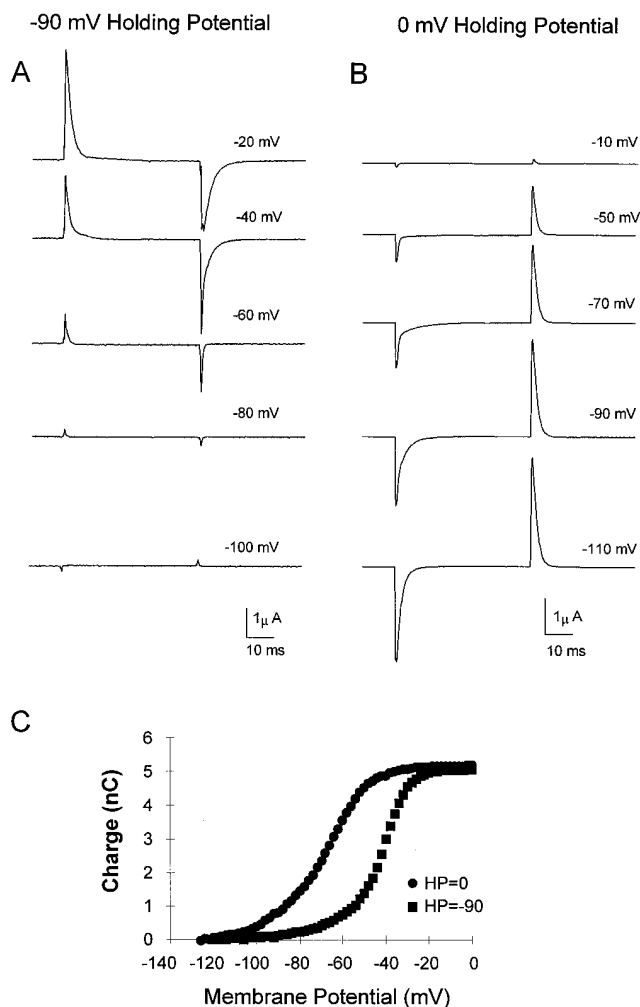1 μA   1 μA
10 ms   10 ms

C

FIGURE 4. Gating currents from −90 and 0 mV HP in the nonconducting mutant *Shaker* Δ-W434F. Same protocol and ionic conditions as in Fig. 3, *A* and *B*. Unsubtracted gating currents from −90 and 0 mV HP, respectively. (*C*) Q-V curve with the absolute charge values. The total charge moved is the same at both HPs. Holding the membrane potential at 0 mV induces an ∼25-mV shift to the more negative potential of the Q-V curve.

Installation of Slow Inactivation

The shift to more negative potentials of the Q-V curve in slow inactivated channels could be explained as the conversion of channels from a "permissive" form (available for activation) to a "reluctant" conformation. In the reluctant (inactivated) conformation, the voltage sensor moves under a different voltage dependence than the permissive conformation. We propose here that the gating charge conversion occurring during long depolarizations is related to the slow inactivation process. To test this hypothesis, we compared the time course of the charge conversion with the time course of the slow inactivation of the current at the same potential. In Fig. 5 *A*, the membrane potential was held at −90 mV for at least 1 min to fully recover all the channels from inactivation. Inactivating prepulses of different duration to 0 mV were applied before a test pulse from 0 to −60 mV. It is clear that the gating current at −60 mV is reduced as the prepulse is made longer (Fig. 5 *A*). To quantify the effect of the prepulse, the integral of the ON gating current normalized to the maximum charge (Fig. 5 *C*, ●) was plotted as a function of the prepulse duration.

As the inactivating prepulse becomes longer, the Q-V curve progressively shifts to the left, approaching the position of the Q-V curve obtained after 1 min at 0 mV HP (steady state) (Fig. 4 *C*, ●). Therefore, the charge reduction reflects the speed of the shift of the Q-V curve in depolarizing conditions. There is no charge reduction, but only a change in its voltage dependence.

To compare the establishment of the charge conversion with the conduction inactivation, we measured the slow decay of the K^+ current due to slow inactivation during 1-min depolarizing pulse at 0 mV in the conducting clone (Fig. 5 *B*). At the end of the pulse, the ionic conductance was reduced by ∼85% due to the slow inactivation. The normalized ionic current decay was plotted (Fig. 5 *C, thick trace*) along with the normalized charge in Fig. 5 *C*. Both processes can be reasonably well fitted simultaneously by the sum of two exponential functions with the same time constants (τ) for ionic and gating current inactivation of 4.1 and 24 s.

Recovery from Slow Inactivation

The recovery of the charge movement and ionic current were measured after a 1-min preconditioning pulse to 0 mV that drove most of the channels into a slow inactivated state. Then, repolarizing pulses of different duration to −90 mV were delivered, allowing different times of recovery at this potential. The recovery of the charge and the ionic current as a function of the duration of the −90 mV pulse was measured with a test pulse from −90 to +20 mV. The recovery of the slow inactivated charge was measured by integrating the ON
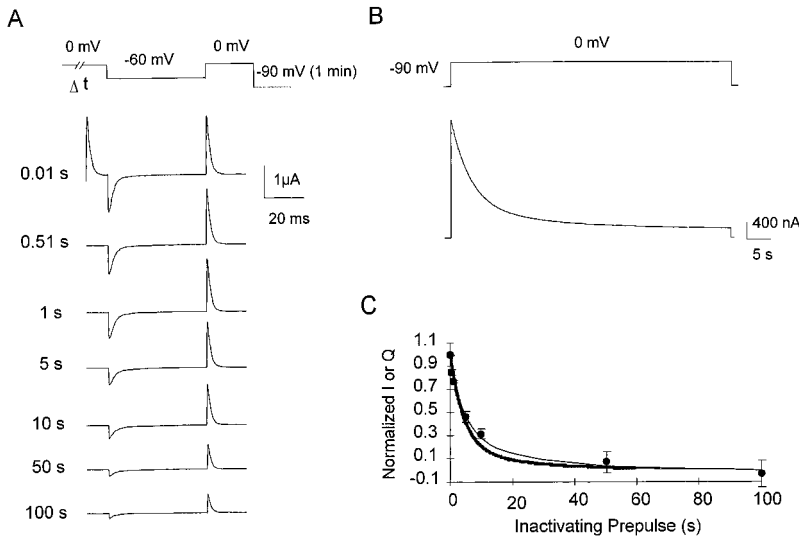
FIGURE 5. Correlation between the time course of installation of C-type inactivation and time course of changes in charge movement. (*A*) *Shaker* H4-Δ-W434F upper trace is the pulse protocol, remaining traces are unsubtracted gating currents. Linear components were analogically compensated with the amplifier transient cancellation at 20 mV HP. Numbers preceding the traces are the duration of the conditioning pulse to 0 mV. The −90 mV HP was held for 1 min between each stimulating pulse to fully recover from the inactivation. Note that increasing the duration of the conditioning pulse to 0 mV induces a reduction in the charge movement measured for a pulse from 0 to −60 mV. (*B*) *Shaker* H4-Δ. Time course of the ionic current during 1-min depolarizing pulse to 0 mV. (*C, symbols*) Normalized charge movement (from 0 to −60 mV, from records of the type shown in *A* as a function of the inactivating prepulse. (*wide trace*) Time course of ionic current during a pulse to 0 mV (as shown in *B*). Data are normalized to their minima and maxima and fitted to the sum of two exponential functions (*narrow trace*) constraining the two time constants to be the same for ionic and gating current data: $\tau_{fast} = 4.1$ s, $\tau_{slow} = 24$ s. The ratios between the fast and slow components for charge movement and ionic current were 2.15 and 3.7, respectively. COVG technique in external isotonic Na-MES. Error bars are SEM ($n = 6$).

gating current during the test pulse. ON gating current increased progressively depending on the duration of the recovery interval (Fig. 6 *A*). In this case, the charge increase reflects the shift towards the right along the voltage axis of the Q-V curve. An identical protocol was used to monitor the recovery of the ionic current (Fig. 6 *B*). As it was described for the installation of slow inactivation, a tight correlation between the time courses of charge and ionic current recovery was found. Experimental points describing the recovery of both charge
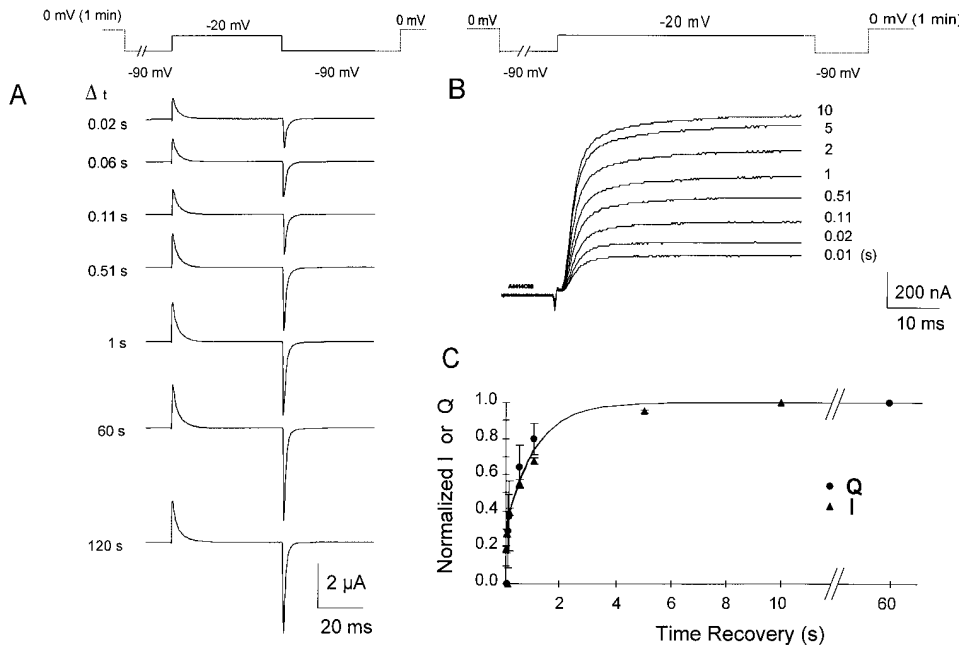

FIGURE 6. Correlation between the time course of recovery of slow inactivation and of changes in charge movement. (*A*) *Shaker* H4-Δ-W434F. Upper trace is the pulse protocol, remaining traces are unsubtracted gating currents. Linear components were analogically compensated with the amplifier transient cancellation at 20 mV HP. Numbers preceding the traces are the duration of the conditioning pulse to −90 mV. The 0 mV HP was held for 1 min between each stimulating pulse to fully slow inactivate the channels. Note that increasing the duration of the conditioning pulse to −90 mV induces an increase of the charge movement measured for a pulse from −90 to −20 mV. (*B*) *Shaker* H4-Δ. Similar protocol as in *A* to investigate the recovery of the ionic current from slow inactivation. Upper trace is the pulse protocol, remaining traces are unsubtracted K⁺ currents for a test pulse from −90 to −20 mV. The durations of the conditioning pulses to −90 mV are shown next to the traces. (*C*) Simultaneous fit to normalized charge movement (from −90 to −20 mV as in *A*) and ionic current during the same voltage step as shown in *B*. Averaged data (●, charge, $n = 3$; and ▲, ionic current, $n = 3$) were fitted to the sum of two exponential functions with the same two time constants but with different amplitudes: $\tau_{fast} = 0.01$ s, $\tau_{slow} = 1.1$ s. The ratios between the fast and slow components for charge movement and ionic current were 0.46 and 0.43, respectively. Data points are normalized to their minima and maxima. COVG technique in external isotonic Na-MES.
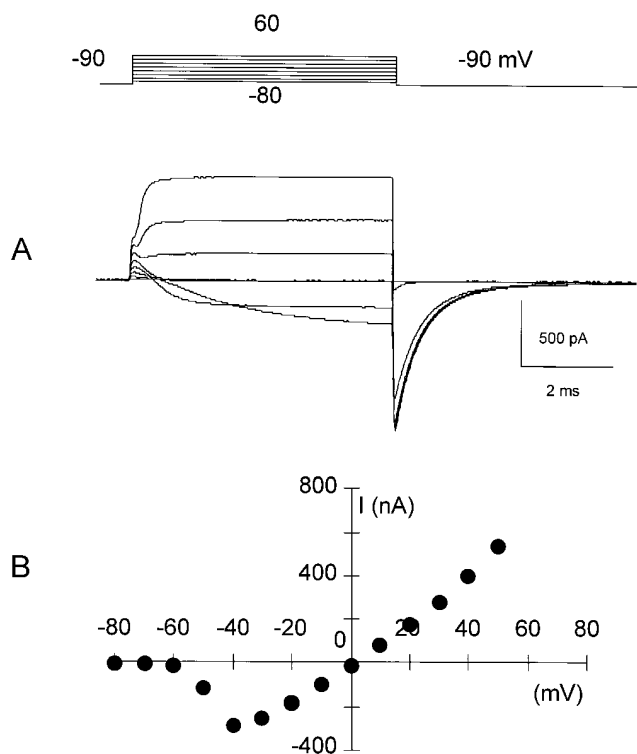
Slow Inactivation in Shaker K⁺ Channels

FIGURE 7. Cs⁺ currents in *Shaker* H4-Δ. (*A*) Membrane currents in cell-attached mode from an oocyte in which the internal medium was equilibrated with isotonic Cs-MES. The pipette was filled with isotonic 2 mM Cs-MES CaCl₂, −90 mV HP. Pulse protocol (*top*): pulses were from −80 to 60 mV in 20-mV increments. Linear components were subtracted with P/−4 protocol from −90 mV subtracting HP. (*B*) I-V relationship from the experiment in *A*. The reversal potential for Cs⁺ is 0 mV.

and ionic current could be well fitted simultaneously to the sum of two exponential functions with the same time constants. The two τ obtained by the fit were 0.01 and 1.1 s (Fig. 6 *C*), indicating that the recovery from slow inactivation at −90 mV in *Shaker* H4-Δ channel is a much faster process than the installation at 0 mV.

We measured the recovery of charge movement and ionic conductance simultaneously in the conducting clone *Shaker* H4-Δ to give further support to the hypothesis that the changes in charge movement are correlated to the slow inactivation of the channel. In this case, we took advantage of the low permeability of *Shaker* H4-Δ channels to Cs⁺ to record at the same time gating and ionic current of the same order of magnitude. Cs⁺ currents were recorded in cell attached patches under symmetrical isotonic Cs-MES in permeabilized oocytes. We confirmed that in external Cs⁺ slow inactivation is still present (López-Barneo et al., 1993). The complete exchange of the internal oocyte medium with the bath solution (isotonic Cs-MES) was checked measuring the reversal potential of the ionic current. Fig. 7 *A* shows the currents elicited under these conditions and Fig. 7 *B* shows the current to volt-
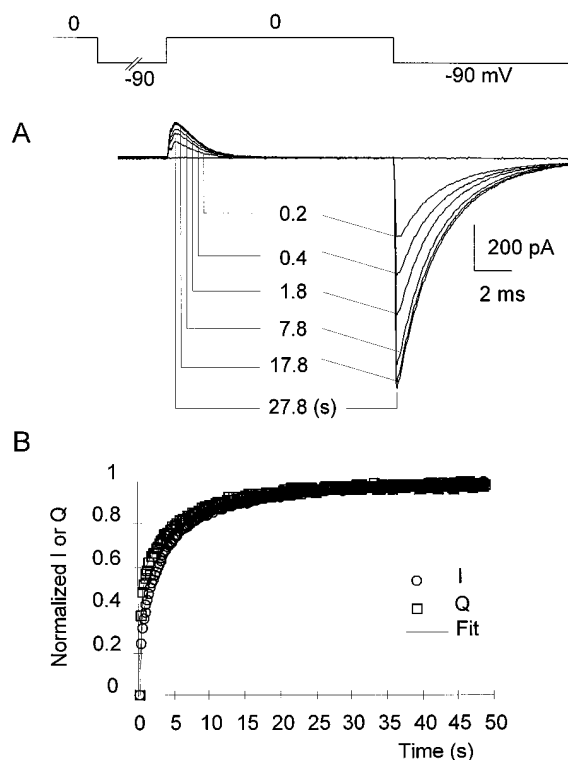

FIGURE 8. Ionic and gating current of *Shaker* H4-Δ recover from slow inactivation with the same course. Same conditions as in Fig. 7. (*A*) Current traces in isotonic Cs-MES obtained pulsing to the reversal potential for Cs⁺ (0 mV). The channels were inactivated at 0 mV for 1 min and recovered with different pulse duration to −90 mV. Note that increasing the duration of the conditioning pulse to −90 mV produces an increase of the charge movement measured for a pulse from −90 to 0 mV, and a parallel increase in the tail current at the repolarizing potential (−90 mV). (*B*) Time course of the recovery of ionic current and gating charge. Simultaneous fit to normalized charge movement (from −90 to 0 mV as in *A*) and peak tail current during the repolarization to −90 mV. Data (ionic current ● and charge ▲, normalized to their minima and maxima) were fitted to the sum of two exponential functions (*continuous line*) with the same time constants and different amplitudes: $\tau_{fast} = 0.28$ s, $\tau_{slow} = 6.47$ s. The ratios between the fast and slow components for charge movement and ionic current were 2.33 and 1.35, respectively.

age (I-V) curve, confirming the symmetry between the internal and the pipette solutions containing isotonic Cs-MES with 2 mM CaCl₂. Pulsing to the reversal potential for Cs⁺ (0 mV in our conditions, see I-V curve in Fig. 7 *B*), the only outward current elicited is the gating current (Fig. 8 *A*) (Noceti et al., 1996). However, at the end of the pulse the driving force for the repolarization to −90 mV favors a large inward Cs⁺ tail current that is proportional to the number of channels open at the end of the depolarizing pulse together with a small contamination of the OFF gating current (Fig. 8 *A*). After a 1-min depolarization to 0 mV, we measured the recovery from inactivation after repolarizations of different duration at −90 mV. The current traces in Fig. 8 *A*
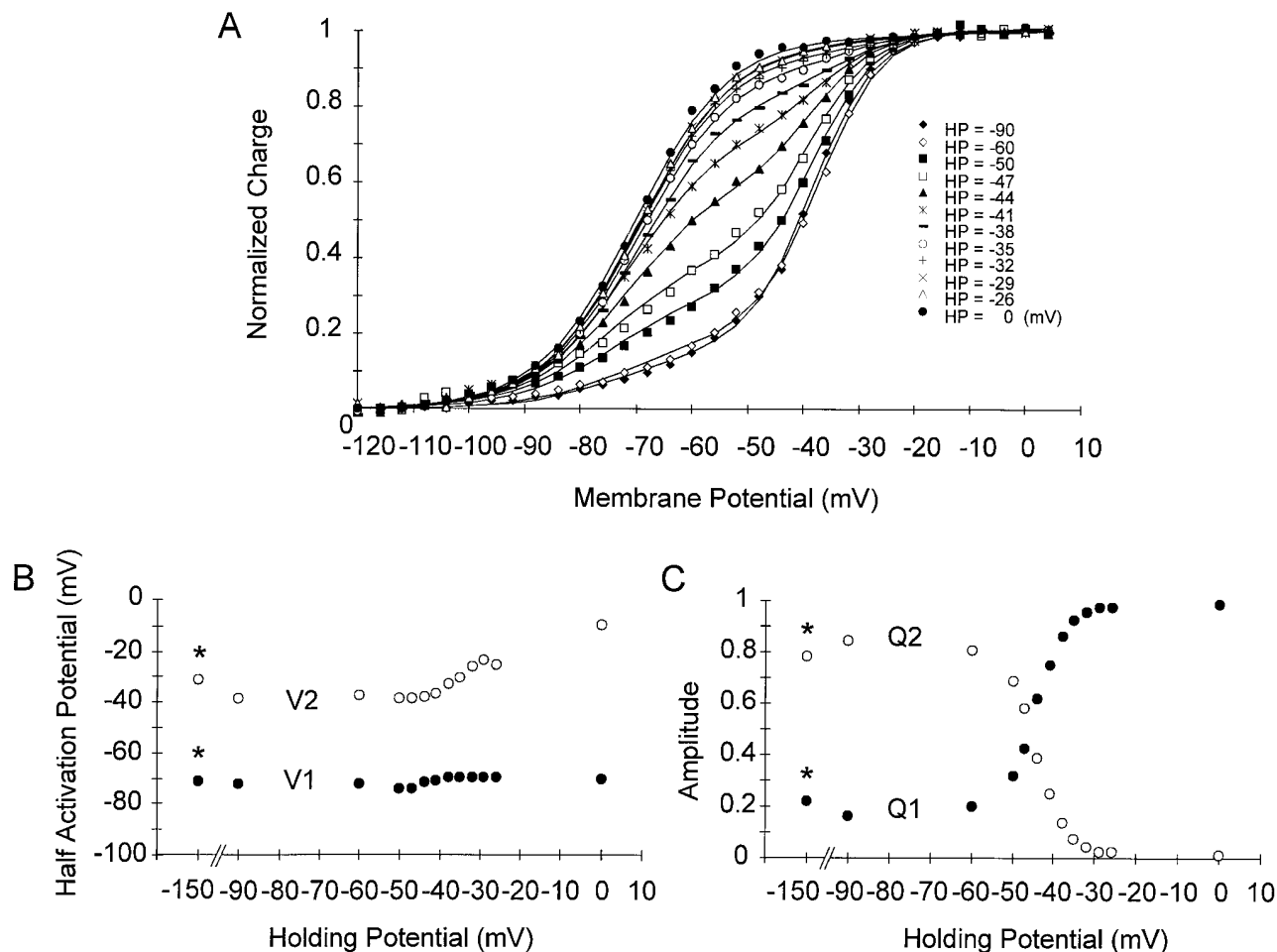
FIGURE 9. Effect of intermediate holding potentials on the charge movement. COVG technique in isotonic Na-MES. (A) Normalized Q(V) curves from the same oocyte obtained from HPs ranging from -90 to 0 mV as indicated. Continuous lines are the fits to a sum of two Boltzmann distributions in the form of: $Q_{on}/Q_{max} = Q_1/Q_{max}/\{1 + \exp[z_1(V_{1half} - Vm)F/RT]\} + Q_2/Q_{max}/\{1 + \exp[z_2(V_{2half} - Vm)F/RT]\}$ where Q_{max} is the maximum charge movement, Q_1 and Q_2 are the amplitudes of the charge components, z_1 and z_2 are the effective valences and V_{1half} and V_{2half}, the respective half activation potentials; F, R, and T are the usual thermodynamic constants. The fitting was performed to obtain the same effective valences (z_1 and z_2) for all the Q-V curves and different amplitude and half activation potentials. The effective valences (z) were 2.9 for the first, more negative component, and 4.4 for the second component of the Q-Vs. The half activation potentials (V_{1half} and V_{2half}) and the amplitudes Q_1 and Q_2 for all the Q-V curves are plotted as a function of the holding potential in B and C, respectively. *Data points are from a different oocyte.

show that both charge movement (transient outward current) and membrane conductance (tail current) recover as the recovering time to -90 mV increases. The time course of the recovery for the charge and the ionic current, plotted in Fig. 8 B, follow a very similar time course. Both recoveries were fitted simultaneously to the sum of two exponential functions with different weights ($\tau_{fast} = 0.28$ s, and $\tau_{slow} = 6.47$ s).

Relative Proportion of the Reluctant and Compliant Components in the Q-V Curves Is a Function of the Holding Potential

We explored the effect of intermediate depolarizations on the voltage dependence of the charge movement.

Holding potentials ranging between -90 and 0 mV were applied to evaluate their effects on the charge movement. The holding potential was maintained for at least 1 min before voltage stepping. Fig. 9 A shows Q-V curves obtained in the same oocyte and at different holding potentials. The gating charge movement was quantified by fitting two Boltzmann distributions (Q_1 and Q_2).

$$Q(V) = Q_1/\{1 + \exp[(V_1 - V)z_1F/RT]\} + Q_2/\{1 + \exp[(V_2 - V)z_2F/RT]\}, \quad (1)$$

where V_1 and V_2 are the midpoints and z_1 and z_2 are the effective valences for gating charge components Q_1 and Q_2, respectively. All the Q-V curves could be simultaneously fitted with the same effective valences, z_1 and z_2, and with different relative amplitudes for the two com-

ponents of the Q-V curves: the best fit gave $z_1 = 2.94$, $z_2 = 4.43$. At hyperpolarized holding potentials more negative than -60 mV, the Q-V curves show a smaller component that corresponds to the movement of Q_1 ($\sim$15–20% of the total charge) with a shallower voltage dependence ($z_1 = 2.94$) and a second larger component (Q_2) with higher voltage dependence ($z_2 = 4.43$) (Stefani et al., 1994). Raising the HP more positive than -50 mV (i.e., increasing the population of the slow inactivated channels), the Q-V curves start shifting toward the left along the voltage axis. The half activation potential (V_1) of Q_1 was $\sim$$-70$ mV for all holding potentials showing a very small sensitivity to the HP, while for Q_2 half activation potential (V_2) was less negative for holding potentials more positive than -40 mV (Fig. 9 B). The changes in the Q-V curves with different holding potentials was mainly due to changes in the relative amplitudes of the components Q_1 and Q_2. Q_1 increased as the HP was made more positive and it reached almost 100% of the amplitude of the total charge movement for HP more positive than -30 mV (Fig. 9 C). At the intermediate holding potentials, between -30 and -50 mV, $\sim$50% of the channels are inactivated (Fig. 2 D), and in this voltage range a clear separation between Q_1 and Q_2 is observed with $\sim$0.5 relative amplitude. The change in relative amplitudes of Q_1 and Q_2 as the HP is made more positive is most economically explained on the basis of an increase in the population of channels that are slow inactivated.

DISCUSSION

Yellen et al. (1994) and Liu et al. (1996) have shown that slow inactivation involves a structural rearrangement of the outer mouth of the *Shaker* K$^+$ channel. Changes in the protein structure are likely expected to modify the position and the mutual interactions of the charged domains inside a folded protein. We have shown in this work that long depolarizations modify the voltage dependence of the gating charge movement and that this change appears to be related to the process of slow inactivation. From a molecular point of view, these results can be interpreted as a conformational change of the voltage sensor induced by the slow inactivation process.

We have shown the correlation between the time course of the changes in voltage dependence of the charge movement and the time course of the inactivation during a long depolarization, as well as the recovery of the ionic current and the recovery of the voltage dependence of the charge after a long depolarization. These data support the hypothesis that slow inactivation involves relatively slow changes in the protein structure under depolarizing potentials that modify the "close → open" pathway, enhancing the energy barrier that the protein must overcome to assume a conduct-

ing conformation. A consequence of prolonged depolarization is probably the development of new interactions of the voltage sensor within the protein. An evidence of this interaction is easily appreciable considering the Q-V curves at 0 and -90 HP in Fig. 3 D: a voltage step from 0 to -60 mV is sufficient to move $\sim$90% of the charge in the noninactivated channel held at -90 HP (Fig. 3 D, ■), but if the channel is maintained at 0 mV for a long time (i.e., slow inactivated), the same voltage step is unable to move charge within the recording period (Fig. 3 D, ●). However, in slow inactivated channels it is possible to move the same amount of total charge, but a voltage step from 0 to $\sim$$-120$ mV is required.

Which Type of Inactivation Process Is Associated with the Change in the Voltage Dependence of the Charge Movement?

In the *Shaker* channel, two types of inactivation have been distinguished on the basis of their structural determinants. A tethered "ball peptide" formed by the first 20 amino acids at the NH$_2$-terminal end of the channel protein is responsible for the so called N-type inactivation. A second type of inactivation has been named C-type because of its sensitivity to mutations in the S6 transmembrane segment (Hoshi et al., 1991). Recently, C-type inactivation has been used as a synonym of slow inactivation. However, mutations in the pore region can modulate the rate of the inactivation process (Labarca and MacKinnon, 1993; López-Barneo et al., 1993; De Biasi et al., 1993). There is no evidence that C-type inactivation and the one originated by mutations in the pore are the same type of inactivation process from a molecular point of view. The designation "P-type" inactivation has been properly introduced by De Biasi et al. (1993) in describing the effect of a point mutation in the pore region (V369K) of Kv2.1 channels. This mutation resulted in a fast inactivation of the ionic current having different characteristics from N- and C-type inactivation.

It has been proposed that the pore mutant *Shaker* W434F is a constitutively C-inactivated channel (Yan et al., 1996). However, we have shown that the W434F mutation has a normal voltage dependence of the charge movement for -90 mV HP and a left shift on the voltage axis of the Q-V curve after long depolarization at 0 mV. If W434F were a C-inactivated channel, we would expect the position of its Q-V curve to be left shifted when the holding potential was -90 mV. Along with this observation, other *Shaker* H4-Δ pore mutants like D447E and D447N + T449V (Seoh et al., 1996) have the same behavior: despite the lack of conduction, in these mutants the position of the Q-V curves at -90 mV HP is normal and left shifted when the membrane is held at 0 mV for prolonged periods of time. This apparent paradox can be easily resolved by assuming that

there are two distinct slow inactivation processes: P- and C-type and that only C-type inactivation is associated with modifications in the voltage sensor conformation that induces shifts in the Q-V curve.

Kinetic Model for the Slow Inactivation

Most of the kinetic and steady state properties shown here for *Shaker* H4-Δ and *Shaker* H4-Δ-W434F can be reproduced by a simple model (Fig. 10 *A*) based on the one presented by Bezanilla et al. (1982) and that accounts for slow inactivation and Q-V shift for the squid axon Na$^+$ channels.

The model is based on an eight-states sequential model (Bezanilla et al., 1994) to which an equal number of inactivated states (I) were added (Fig. 10 *A*). The elementary rates connecting the upper and the lower rows of states, γ and δ, are voltage independent and much smaller than the rates connecting the states of the normal and inactivated modes. Thus, the channel gates with voltage in two modes: the normal mode (Fig. 10 A, *upper row*), and the inactivated mode (Fig. 10 A, *lower row*). The main assumption of this model is that the inactivated states are more stabilized as the channel progresses toward the open state. Specifically, this stabilization has been modelled as an interaction with energy $W = w/kT$ that is the same in each of the transitions in the lower row. This interaction energy increases the forward rates between the inactivated states by a factor equal to exp(W), and the resulting equilibrium constants are represented in the figure as $K_i$exp(W), where i is the state index. Microscopic reversibility requires that the return rates between the inactivated and normal states will be multiplied by exp(Σ$_i$W$_i$), stabilizing the inactivated states in proportion to the proximity of the open state. It is then easy to see that a positive holding potential will stabilize the rightmost inactivated state, and that under these conditions a short repolarization will have a leftward shift of the Q-V curve because the forward rates are increased by a factor exponentially dependent on the interaction energy. When the membrane is extremely hyperpolarized, the channels will be preferentially in the normal mode (δ exp[7W] >> γ). The relatively small value of the interaction energy (∼2.4 kT) could be interpreted in molecular terms as a small and slow conformational change that affects the energy profile encountered by the voltage sensor. Thus, depolarized potentials maintained for prolonged periods of time make the return of the voltage sensor to the resting position more unlikely.

For long and strong depolarizations, the relatively slow population of the inactivated state connected to the open state produces the slow decay of the ionic current. From the inactivated state connected to the open state, the transition back to the open state becomes very unlikely due to the small backward rate constant of
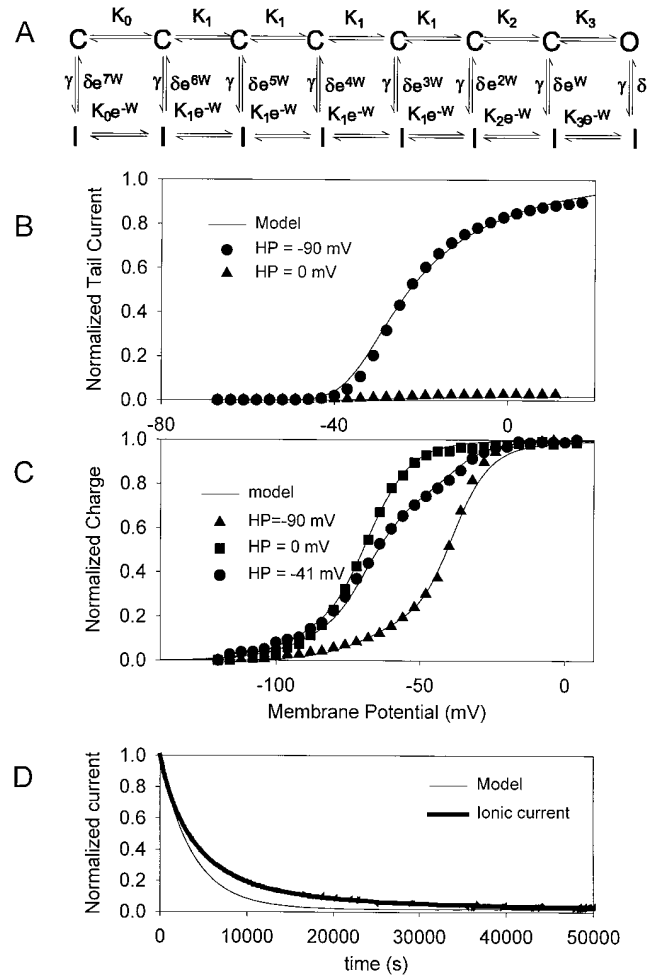

FIGURE 10. Minimum model fitting the main properties of *Shaker* H4-Δ K$^+$ channel. (*A*) Modified sequential model (Bezanilla et al., 1994) with an additional eight inactivated (I) states. Steady state and kinetic properties were fitted simultaneously to this model. (*B*) The result from the fitting is given for the G-V curves obtained from −90 and 0 mV HP and (*C*) for the charge movement measured from holding potentials −90, −41, and 0 mV. The fit (*thin line*) for the time course of the inactivation of the ionic current at 0 mV is shown in *D*. The value of the parameters used were: equilibrium constants: $K_0 = 0.00093$, $K_1 = 0.03559$, $K_2 = 0.03649$, $K_3 = 0.1912$; valences (e_0): $z_0 = 2.55$, $z_1 = 2.0_1$, $z_2 = 2.87$, $z_3 = 1.27$; inactivation rates (s^{-1}): γ = 0.00026, δ = 4.22 × 10^{-6}; interaction energy (kT units): W = 2.427.

this transition. After the channel has reached the slow inactivated state, fast repolarizations produce charge movement that reflects the transition among the inactivated states. The transition I → C becomes energetically more probable at hyperpolarized potentials. The new voltage dependence of the slow inactivated charge (experimentally corresponding to the left shifted Q-V curve at depolarized holding potentials) corresponds to the charge movement related to the transitions among the inactivated states in the lower line of the proposed model. For hyperpolarized holding potentials, where no significant slow inactivation is present, the Q-V

curve is generated by the charge moving in the transitions occurring between the closed states.

The kinetic model shown in Fig. 10 *A* was sufficient for describing the features of the G(V) curves from different holding potentials (Fig. 10 *B*) and it predicts the position of the Q-V curves measured from −90-, 0-, and −41-mV holding potentials. Fig. 10 *D* shows the time course of the ionic current after a depolarization step to 0 mV (*thick line*) and the prediction of the kinetic scheme given in Fig. 10 *A*. The model fails to give an adequate description of the second slow component of the recovery from slow inactivation. This is an indication that the inactivation process may occur in more than one transition. This would add another parallel line of inactivated states that would make the model complicated and difficult to test experimentally.

REFERENCES

Armstrong, C.M., and F. Bezanilla. 1977. Inactivation of the sodium channel. II. Gating current experiments. *J. Gen. Physiol.* 70:567–590.

Bezanilla, F., R.E Taylor, and J.M., Fernandez. 1982. Distribution and kinetics of membrane dielectric polarization. I. Long-term inactivation of gating currents. *J. Gen. Physiol.* 29:21–40.

Bezanilla, F., E. Perozo, D.M. Papazian, and E. Stefani. 1991. Molecular bases of gating charge immobilization in *Shaker* potassium channel. *Science (Wash. DC).* 254:679–683.

Bezanilla, F., E. Perozo, and E. Stefani. 1994. The gating of *Shaker* K+ channels. II. The components of gating currents and a model of channel activation. *Biophys. J.* 66:1011–1021.

Choi, K.L., R.W. Aldrich, and G. Yellen. 1991. Tetraethylammonium blockage distinguishes two inactivation mechanisms in voltage-activated K+ channels. *Proc. Natl. Acad. Sci. USA.* 88:5092–5095.

De Biasi, M., H.A. Hartmann, J.A. Drewe, M. Taglialatela, A.M. Brown, and G.E Kirsh. 1993. Inactivation determined by a single site in K+ pores. *Pflugers Archiv. Eur. J. Physiol.* 4224:335–363.

Ehrenstein, G., and D.L. Gilbert. 1966. Slow changes of potassium permeability in the squid giant axon. *Biophys. J.* 6:553–566.

Fedida, D., R. Bouchard, and F.S.P. Chen. 1996. Slow gating charge immobilization in the human potassium channel Kv 1.5 and its prevention by 4-aminopyridine. *J. Physiol. (Camb.).* 494:377–387.

Hodgkin, A.L., and A.F. Huxley. 1952. A quantitative description of membrane current and its application to conduction and excitation in nerve. *J. Physiol.* (Camb.). 117:500–544.

Hoshi, T., W.N. Zagotta, and R.W. Aldrich. 1990. Biophysical and molecular mechanisms of *Shaker* potassium channel inactivation. *Science (Wash. DC).* 250:533–538.

Hoshi, T., W.N. Zagotta, and R.W. Aldrich. 1991. Two types of inactivation in *Shaker* K+ channels: effects of alterations in the carboxy-terminal region. *Neuron.* 7:547–556.

Kamb, A., L.E. Iverson, and M.A. Tanouye. 1987. Molecular characterization of Shaker, a *Drosophila* gene that encodes a potassium channel. *Cell.* 50:405–413.

Labarca, P., and R. MacKinnon. 1993. Permeant ions influence the rate of slow inactivation in *Shaker* channels. *Biophys. J.* 61:A378.

Liu, Y., M.E. Jurman, and G. Yellen. 1996. Dynamic rearrangement of the outer mouth of a K+ channel during gating. *Neuron.* 16:859–867.

López-Barneo, J., T. Hoshi, S.F. Heinemann, and R.W. Aldrich. 1993. Effects of external cations and mutations in the pore region on C-type inactivation of *Shaker* potassium channels. *Receptors Channels.* 1:61–71.

Noceti, F., P. Baldelli, X. Wei, N. Qin, L. Toro, L. Birnbaumer, and E. Stefani. 1996. Effective gating charges per channel in voltage dependent K+ and Ca²+ channels. *J. Gen. Physiol.* 108:143–155.

Ogielska, E.M., W. Zagotta, T. Hoshi, S.H. Heinemann, J. Haab, and R. Aldrich. 1995. Cooperative subunit interactions in C-type inactivation of K channels. *Biophys. J.* 69:2449–2457.

Olcese, R., L. Toro, E. Perozo, F. Bezanilla, and E. Stefani. 1994. Prolonged depolarization changes charge movement properties in Shaker-IR W434F K+ channel. *Biophys. J.* 66:A107.

Olcese, R., L. Toro, F. Bezanilla, and E. Stefani. 1995. Correlation between charge movement and ionic current during C-type inactivation in Shaker-IR potassium channels. *Biophys. J.* 68:A33.

Panyi, G., Z. Sheng, L. Tu, and C. Deutsch. 1993. C-type inactivation of voltage gated K channel occurs by a cooperative mechanism. *Biophys. J.* 69:896–906.

Perozo, E., R. MacKinnon, F. Bezanilla, and E. Stefani. 1993. Gating currents from a non-conducting mutant reveal open-closed conformations in *Shaker* K+ channels. *Neuron.* 11:353–358.

Seoh, S.-A., D. Starace, D.M. Papazian, E. Stefani, and F. Bezanilla. 1996. D447N and W434F mutations in the pore of Shaker B K+ channels prevent ion conduction but restore conducting states by combined mutation with T449Y. *Biophys. J.* 70:A190.

Stefani, E., L. Toro, E. Perozo, and F. Bezanilla. 1994. The gating of *Shaker* K+ channels. I. Ionic and gating currents. *Biophys. J.* 66:996–1010.

Yan, Y., Y. Yang, and F.J. Sigworth. 1996. How does W434F block *Shaker* channel current? *Biophys. J.* 70:A190.

Yellen, G., D. Sodickson, T.S. Chen, and M.E. Jurman. 1994. An engineered cysteine in the external mouth of a K+ channel allows inactivation to be modulated by metal binding. *Biophys. J.* 66:1064–1075.

Zagotta, W.N., T. Hoshi, and R.W. Aldrich. 1989. Gating of single *Shaker* K channels in Drosophila muscle and in Xenopus oocytes injected with *Shaker* mRNA. *Proc. Natl. Acad. Sci.* USA. 86:7243–7247.

Zagotta, W.N., T. Hoshi, and T. Aldrich. 1990. Restoration of inactivation in mutants of *Shaker* potassium channels by a peptide derived from ShB. *Science (Wash. DC).* 250:568–571.